Voronoi-Delaunay analysis of normal modes in a simple model glass

V. A. Luchnikov,[1,2] N. N. Medvedev,[1] Yu. I. Naberukhin,[2] and H. R. Schober[2]
[1]*Institute of Chemical Kinetics and Combustion, 630090 Novosibirsk, Russia*
[2]*Theorie III, Institut für Festkörperforschung, Forschungszentum Jülich, D-52425 Jülich, Germany*
(Received 10 February 2000)

We combine a conventional harmonic analysis of vibrations in a soft-sphere glass with a Voronoi-Delaunay geometrical analysis of the structure. ''Structure potentials'' (tetrahedricity, sphericity, or perfectness) are introduced to describe the shape of the local atomic configurations (Delaunay simplices) as a function of the atomic coordinates. Apart from the highest and lowest frequencies the amplitude weighted ''structure potential'' varies only little with frequency. The movement of atoms in soft vibrational modes causes transitions between different ''perfect'' realizations of local structure. As for the potential energy a dynamic matrix can be defined for the ''structure potential.'' Its expectation value with respect to the vibrational modes increases nearly linearly with frequency and shows a clear indication of the boson peak. The structure eigenvectors of this dynamical matrix are strongly correlated to the vibrational ones. Four subgroups of modes can be distinguished.

I. INTRODUCTION

The thermodynamic properties of glasses at low temperatures differ from those of the corresponding crystals.[1] At low temperatures the specific heat is strongly enhanced compared to the Debye contribution stemming from the sound waves. The excitations underlying this enhancement have been shown to be two-level systems below $T \approx 1$ K and almost harmonic vibrations above. The vibrational density of states $Z(\nu)$, plotted as $Z(\nu)/\nu^2$ has a maximum, typically near 1 THz, the boson peak.

This low-temperature/low-frequency behavior can be described by the soft potential model.[2,3] In this model one assumes that one common type of structural unit is responsible for the excess excitations. An effective potential describing the motion of this unit is introduced. Depending on the parameters this potential is a single or a double well. In the first case it describes a low-frequency localized vibration and, in the second, tunneling through the barrier (two-level systems) or relaxation over the barrier. For low energies a general form for the distribution of the parameters describing the effective potentials can be given. Fitting this model to the experimental data, one finds that 20–100 atoms or molecular units move collectively both in the tunneling and in the localized vibrations.[4,5] It should be emphasized that the concept of low-frequency localized vibrations is an idealization. These modes will always interact with the sound waves of similar frequency and, therefore, also between each other. This delocalizes the modes and they are only quasilocal or resonant. Due to level repulsion, for sufficiently high densities of these modes, the interaction will change their density of states from $Z(\nu) \propto \nu^4$ to $Z(\nu) \propto \nu$ thus creating the boson peak.[6] Such a model does not, however, specify the physical nature of the localized modes or their origin in different types of glasses.

In computer simulations of a soft sphere glass (SSG) quasilocalized vibrations centered on ten and more atoms have been observed.[7] These quasilocalized modes can be seen as the core of resonant modes in an infinite system. As is typical for such modes, they couple bilinearly to the sound waves that become damped. This is a purely harmonic interaction. Near the boson peak the interaction is so strong that the Ioffe-Regel limit is reached for the sound waves and the mean free path drops to the wavelength. The modes comprising the boson peak can, however, still be described by a basis of sound waves and soft localized modes.[8] These latter modes are closely related to the local relaxations in the glass and have predominantly a chainlike structure.[9,10] They are centered at atoms whose structural surrounding differs substantially from the average but are not simply regions of low density. From low-frequency Raman scattering a one-dimensional geometry of the boson peak modes was concluded, in agreement with the above picture.[11] In their simulations on amorphous silicon, Fabian and Allen[12] found anomalously large Grüneisen constants of the resonant modes, again pointing towards some distinct structural features causing them.

Quasilocalized low-frequency vibrations have also been observed in computer simulations of numerous other materials, such as, e.g., SiO_2,[13] Se,[14] Ni-Zr,[15] Pd-Si,[16] NiB,[17] in amorphous ice,[18] and in amorphous and quasicrystalline Al-Zn-Mg.[19]

However, the above explanation of the boson peak being due to the interaction of localized (resonant) modes and extended modes (sound waves) is not universally accepted. Some authors ascribe the boson peak to low-lying optic bands that hybridize with the acoustic states,[20] or to low-lying acoustic branches decorated with a random component,[21] or to spatial damping of sound waves due to density fluctuations.[22]

At frequencies above the boson peak the vibrational eigenmodes have a rather complicated structure. They are strongly delocalized but not propagating. This behavior is described by the term ''diffusons'' introduced by one group.[23] From the dynamic structure factor one can still define dispersion curves for these modes, both from experiment[24,25] and from simulation.[20,26] This can also be observed in the soft-sphere glass studied in this paper (un-

published results). The interpretation of these dispersion curves and especially the damping are still controversial. Finally, at the highest frequencies or near-gaps of the spectrum truly localized modes are observed.

As seen already from our previous remarks, there is a great deal of literature connecting the vibrational properties, and in particular the boson peak, with structural properties. The local dynamics in the amorphous state is often connected with the so-called medium-range order in glasses.[27,28]

In another line of reasoning, soft modes and the boson peak are connected with the concept of frustration and local strains, see, e.g., Ref. 29. It was argued that below the glass transition the remaining free volume would collapse leaving centers of internal strains.[30] These structural defects can serve as centers of relaxations and soft vibrations. On a similar line local pressures were defined that are then related to local force constants.[31]

Going one step further one considers frustration as resulting from a competition between different structures, or between local and global dense packing. For three-dimensional simple sphere models global dense packing results in fcc or hcp structures, whereas, locally icosahedral packings are the most dense. However, the latter are not space filling. Investigations to find the most dense close packing of hard spheres are still pursued.[32] It seems that random packings cannot exceed a packing fraction $f_{\mathrm{pack}} \approx 0.645$ considerably below the value for the ordered structures, $f_{\mathrm{pack}} \approx 0.74$. This difference is related to the degeneracy between the fcc and hcp structures leading to a geometrical frustration associated with the impossibility to fill the space with perfect tetrahedra.[33] Frustration of local packings, in particular in binary system, have been utilized to derive criteria for the glass transition and melting, see, Ref. 34, and references therein. As a quantitative measure of randomness atomic stresses were introduced.

Related to this frustration picture is the hypothesis on the origin of the soft mode, that the most active atoms oscillate between neighboring minima of the potential energy formed by a cage of surrounding atoms.[35] These minima correspond to some more ''perfect'' local arrangements of the atoms. The coupling to the rest of the material changes this double-well system to one of a soft single well. One example for such a situation is the interstitial atom in an fcc metal. A medium-sized interstitial occupies the octahedral site. Increasing the size of the interstitial atom the octahedral site becomes unstable and the interstitial moves to an off-center position. The impeding instability is indicated by low-lying resonance vibrations.[36,37] The instability in this example is caused by a local compression that causes the simultaneous occurrence of resonant low-frequency and localized high-frequency vibrations. In the glass the modes are more extended, typically consisting of string-like groups of some 20 atoms.[8] Instead of the single interstitial atom one has to take a group of atoms and, due to the lacking symmetry, the energy minima will be shifted relative to each other. Keeping this in mind the underlying mechanism can still be true. The simultaneous occurrence of low- and high-frequency localized modes centered on one atom has indeed been observed.[7]

Some of the present authors[38,39] recently introduced a parameter of ''perfectness'' and have shown that a computer model of amorphous argon has, on a nanometer scale, a heterogeneous structure containing regions of more ''perfect'' or ''imperfect'' atomic arrangements. In the regions of perfect structure the elementary packings of four neighboring atoms (the Delaunay simplices) are close to either regular tetrahedra or quart-octahedra,[38] i.e., quarters of regular octahedra. In the regions of imperfect structure the local configurations of the neighboring atoms differ markedly from these ideal shapes. A partial spectrum of the vibrational states of the atoms in the regions of more ''imperfect'' structure displays an excess of low-frequency modes.[39]

In the present paper we want to verify and substantiate this notion for the SSG and to investigate the correlations between the vibrations in the whole frequency range with different parameters characterizing local perfectness. For this purpose we combine the harmonic analysis of Ref. 7 with the Voronoi-Delaunay geometrical description of the local structure used in Ref. 39. First, we shift the atoms of the model along the eigenvector of a low-frequency quasilocalized normal mode and observe the changes in the local atomic arrangements caused by the shift. This allows us to visualize the specific transformations of the local structure that accompany the motion of the atoms in the vibrations. In a next step we calculate the atomic perfectness weighted with the squared amplitudes of the vibrational modes. This quantity varies only weakly with frequency. Considering that the vibrations are connected with changes in the geometry, we introduce a ''structural dynamical matrix.'' We will show in the following that there is a strong correlation between the ''structural eigenvectors'' and their vibrational counterparts. This correlation divides the vibrations, as regards structure changes, into separate classes: longitudinal and transverse extended, high-frequency localized, and low-frequency quasilocalized modes.

II. THE SOFT-SPHERE GLASS

We use 55 glassy configurations of 500 atoms each, interacting via a soft-sphere pair potential

$$u(r) = \epsilon\left(\frac{\sigma}{r}\right)^6 + A\left(\frac{r}{\sigma}\right)^4 + B. \tag{1}$$

To simplify the simulation the potential is cut off at $r/\sigma = 3.0$ and shifted by a polynomial with $A = 2.54 \times 10^{-5}\epsilon$ and $B = -3.43 \times 10^{-3}\epsilon$.

We used the configurations obtained during our earlier work concerning soft quasilocalized modes and local relaxations.[7,10] There, we did a molecular-dynamics simulation with a fixed atomic density, $\rho/\sigma^3 = 1$, periodic boundary conditions, using the Verlet algorithm with temperature scaling, and a time step of 0.04 in units of $m\sigma^2/\epsilon^{1/2}$. The configurations were obtained by a quench from a liquid at about 2.5 times the melting temperature to a reduced temperature of $kT = 0.04\epsilon$ about 5% of the glass transition temperature. The quench rate was about $0.15k/(m\sigma^2\epsilon)^{1/2}$. This rate is close to the ideal quenching rate for this material.[40] After the quench, each sample was aged for several 1000 time steps to stabilize the potential energy and to avoid spurious minima. The final quench to $T = 0$ was done by steepest descent conjugate gradient minimization of the potential energy. From the pair correlation one finds a nearest-neighbor distance of around 1.1σ. For more details see Refs. 7 and 10. The small

size of $N=500$ has the advantage that the lowest quasilocalized modes are seen as localized modes since the cutoff in q values compatible with periodicity excludes the sound waves of similar frequency. In the previous work we have shown that these low-frequency localized modes are the resonant part of the low-frequency modes in larger samples.[8]

The inverse sixth-power potential is a well-studied theoretical model that mimics many of the structural and thermodynamic properties of bcc forming melts including the existence, in its bcc crystal form, of very soft shear modes.[41] In the glassy structure one finds a boson peak with a maximum near $\nu=0.1(\epsilon/m\sigma^2)^{1/2}$ extending to about $\nu=0.4(\epsilon/m\sigma^2)^{1/2}$. The enhancement of the vibrational density of states over the Debye value is by a factor of about 2.5. (Ref. 8)

As before, the frequencies and eigenvectors of normal vibrations are calculated by the diagonalization of the force constant matrix. Imaginary frequencies are absent in the spectrum because the system is in an absolute local minimum of potential energy. For the given number of atoms the minimal q value for sound waves is $q_{\min}=0.79\sigma^{-1}$ giving minimal frequencies of 0.18 and $0.62(\epsilon/m\sigma^2)^{1/2}$ for the transverse and longitudinal sound waves, respectively. Resonant modes with frequencies well below $0.18(\epsilon/m\sigma^2)^{1/2}$ will, therefore, be seen as low-frequency localized modes. This is reflected in the participation ratios given in Ref. 7. One finds proper localized modes at frequencies $\nu>2(\epsilon/m\sigma^2)^{1/2}$ and (quasi) localized low-frequency modes with $\nu<0.2(\epsilon/m\sigma^2)^{1/2}$. The great majority of modes ($0.2<\nu<2$) extends over the system. These latter modes have been called ''diffusons''[23] due to their nonpropagating character. Nevertheless, for the SSG as for other systems, it is possible to extract some very broad ''phonon dispersions'' via the dynamic structure factor.[42]

The SSG was used in extensive studies of the influence of the quench rate on the glass structure.[43,40] In these studies the Voronoi method was used to identify pentagonal rings that can be used as signature of icosahedral packing.

III. VORONOI-DELAUNAY DESCRIPTION OF LOCAL STRUCTURE.

By definition, the *Voronoi polyhedron* (VP) of an atom is that region of space that is closer to the given atom than to any other atom of the system. A dual system spanning space is formed by the *Delaunay simplices* (DS). These are tetrahedra formed by four atoms that lie on the surface of a sphere that does not contain any other atom. Both VP and DS fill the space of the system without gaps and overlaps. In our calculations we do a Voronoi-Delaunay tessellation of the glass configurations by the algorithm described in Ref. 44.

It was found earlier that two main types of DS are predominant in monoatomic glasses,[45,46] namely, DS similar to ideal tetrahedra and DS resembling a quarter of a regular octahedron (quart-octahedron). Following Ref. 46 we introduce as quantitative measure of the deformation from an ideal tetrahedron the *tetrahedricity* of a DS

$$T=\sum_{i<j}\frac{(l_i-l_j)^2}{15\overline{l}^2}, \tag{2}$$

where i and j designate the edges of the simplex, and $\overline{l}$ is the average edgelength. This measure was constructed to be zero for ideal tetrahedron and to increase with distortion. For computational reasons we slightly modify the previous measure of the deviation from an ideal quart-octahedron, the *octahedricity*, using

$$O=\left\{\sum_{m=1}^{6} g_m O_m^{-1}\right\}^{-1}, \tag{3}$$

where

$$g_m=\frac{e^{3\delta_m/\sigma}}{\sum_{i=1}^{6} e^{3\delta_i/\sigma}}, \quad \delta_m=\frac{l_m-\overline{l}}{\overline{l}}, \quad \sigma=\left[\frac{1}{6}\sum \delta_m^2\right]^{1/2},$$

and

$$O_m=\sum_{i<j;i,j\neq m}\frac{(l_i-l_j)^2}{10\overline{l}^2}+\sum_{i\neq m}\frac{(l_i-l_m/\sqrt{2})^2}{5\overline{l}^2}. \tag{4}$$

In a perfect quart-octahedral DS one edge is $\sqrt{2}$ times larger than the other edges. In the previously used measure,[47] it was assumed that the mth edge is the longest. The modified expression Eq. (3) weights the six possible values O_m in such a way that the smallest one dominates. The octahedricity thus tends to zero when the DS is close to a perfect quart-octahedron. This weighting allows us to avoid the use of logical functions for the selection of the maximal edge and guarantees differentiability that is essential for our investigation. For the relevant low values of O, i.e. simplices close to the quart-octahedral shape, our expression reproduces the values of the original definition.

The tetrahedral and quart-octahedral DS can be unified in one class of ''perfect,'' or ''ideal'' simplices.[38] We measure the *perfectness* of the DS shape by

$$S=\left[g_T\left(\frac{T}{T_c}\right)^{-1}+g_O\left(\frac{O}{O_c}\right)^{-1}\right]^{-1}, \tag{5}$$

where

$$g_T=\frac{e^{-3T/T_c}}{e^{-3T/T_c}+e^{-3O/O_c}}, \quad g_O=\frac{e^{-3O/O_c}}{e^{-3T/T_c}+e^{-3O/O_c}}.$$

S tends to zero when the simplex takes the shape of an ideal tetrahedron *or* quart-octahedron. Contrary to the expression proposed in Ref. 38 our measure is differentiable with respect to the atomic coordinates. The relative weights of tetrahedricity and octahedricity, $T_c=0.016$, $O_c=0.033$, are taken from Ref. 47, where they were proposed as boundary values for perfect tetrahedra and perfect quart-octahedra, respectively. The relation of the values T, O to the distortion of a DS can be seen also from the values $T_O\simeq 0.050$ of the tetrahedricity of an ideal quart-octahedron and $O_T\simeq 0.084$ octahedricity of an ideal tetrahedron.

Each atom in the glass is corner of approximately 24 DS. The structural environment of an individual atom can be characterized by the average *perfectness* of these DS:[39]

TABLE I. Values of perfectness, tetrahedricity, and sphericity for an atom in an ideal fcc lattice at the center of an icosahedron and for the glass, averaged according to Eq. (9).

	$\langle S_{\text{atomic}}\rangle$	$\langle T_{\text{atomic}}\rangle$	$\langle \mathcal{S}_{\text{atomic}}\rangle$
fcc lattice	0.0	0.039	0.346
icosahedron	0.095	0.0015	0.325
SSG	0.66 ± 0.17	0.023 ± 0.005	0.358 ± 0.025

$$S_{\text{atom}}=\frac{1}{n_{DS}}\sum_{i=1}^{n_{DS}} S_i, \tag{6}$$

where n_{DS} is the number of DS surrounding the atom.

Another widely used measure of the atomic neighborhood is the *sphericity* of the Voronoi cell:

$$\mathcal{S}=\frac{1}{36\pi}\frac{F^3}{V^2}-1. \tag{7}$$

Here F is the surface area of the VP, and V is its volume. This measure is minimal for a sphere, $\mathcal{S}=0$, and again increases with distortion.

In analogy to the potential energy one can take the total tetrahedricity, perfectness, or sphericity to characterize the structure. We introduce an average ''structure potential'' by

$$\langle T\rangle=\frac{1}{N_{DS}}\sum_{i=1}^{N_{DS}} T_i, \tag{8}$$

and analogously $\langle S\rangle$ and $\langle \mathcal{S}\rangle$, where N_{DS} is the number of DS in the system. Since dynamics is concerned with the motion of the atoms it is often more useful to average over the atomic quantities defined by Eq. 6,

$$\langle T_{\text{atomic}}\rangle=\frac{1}{N}\sum_{i=1}^{N} T_{\text{atomic}}. \tag{9}$$

However, both definitions give similar values.

In Table I we compare the values of the three measures for an ideal fcc structure, an icosahedron, and our glass. The values of the glassy structure clearly deviate from the ones of both ideal configurations. It is, however, not possible to define unambiguously a nearness to either structure using these measures.

IV. SOFT VIBRATIONS AND LOCAL STRUCTURE

Considering the relationship between local structure and soft vibrations one normally looks for peculiarities of atomic arrangements that induce the softness of some low-frequency modes. In the following section we study this relationship from the opposite point of view. Knowing the eigenvector of a vibration (obtained by diagonalization of the force constants matrix) we analyze how the local structure is affected by the collective motion of the atoms along the normal coordinate of the vibration.

We illustrate this for an example of a quasilocalized soft mode. The atoms are shifted along the direction of the $3N$-dimensional, normalized eigenvector $\mathbf{e}$ according to

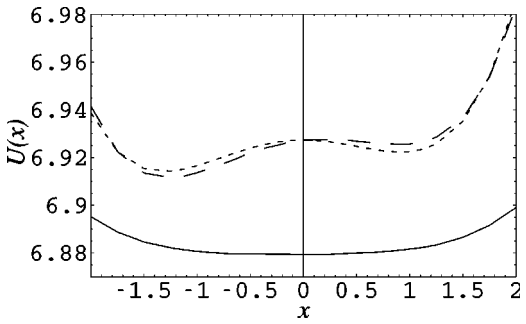

FIG. 1. Average potential energy of atoms in a single soft mode with frequency $\nu=0.0985$, participation ratio $p=0.23$. Solid line, $\langle U(x)\rangle_{\text{tot}}$, potential energy averaged over *all* atoms in the system. Dashed line, $\langle U(x)\rangle_{\text{core}}$, the *partial* potential energy averaged over 61 atoms of the core of the mode. Dotted line, least squares fit of the partial potential energy by a soft potential polynomial $U^*(x)=Ax^2+Bx^3+Cx^4+\langle U(0)\rangle_{\text{core}}$.

$$\mathbf{R}^n(x)=\mathbf{R}_0^n+x\mathbf{e}^n, \tag{10}$$

where $\mathbf{R}_0^n$ is the equilibrium position of atom n. For simplicity we have not normalized the amplitude x to an effective atomic amplitude as is usually done in the soft potential model.

In Fig. 1 the average potential energy per atom, $\langle U(x)\rangle_{\text{tot}}$ (solid line), is shown as a function of the displacement along a single soft eigenmode. This is one of the soft potentials that are described by the soft potential model,[2,3] as has been discussed in the Introduction. The subscript ''tot'' indicates that the averaging is over all 500 atoms of the system. Figure 1 corresponds to a very-well-localized soft mode with $\nu=0.098(\epsilon/m\sigma^2)^{1/2}$, participation ratio 0.23. These values would guarantee a very narrow resonance in the infinite medium.[36]

As mentioned in the Introduction, it has been speculated that the soft modes in glasses originate from some ''soft'' atomic configurations where, in the extreme case, the atoms are stabilized by the embedding matrix in a position lying between minima of the potential energy given by its near neighbors. To illustrate this, we show in Fig. 1 by the dashed line the average potential energy of the 61 atoms that are most active in the given mode, $\langle U(x)\rangle_{\text{core}}$. Atoms are considered as active in a given mode if their amplitude $|\mathbf{e}^n|$ is at least 30% of the maximal atomic amplitude in the mode. We will call these active atoms the *core* of the mode (subscript core). For the modes with participation ratios $p<0.25$ the average number of atoms in their respective cores is 51. The results presented below do not depend strongly on the cutoff used for selecting the active atoms. The *partial* potential energy of the core atoms is indeed double-well shaped with minima at $x_{\text{m}}\approx\pm1.3$, which corresponds to maximal displacements of individual atoms by $|\mathbf{R}^n-\mathbf{R}_0^n|\approx0.2$–$0.3\sigma$ from the equilibrium configuration. This maximal atomic displacement is of the order of the one observed in local low-temperature relaxations.[10]

To obtain a quantitative analysis of the dependence of the partial potential energy on the displacement x, we did a least-square fit of $\langle U(x)\rangle_{\text{core}}$ by the soft potential expression[2–4]

$$U^*(x)=Ax^2+Bx^3+Cx^4+\langle U(0)\rangle_{\text{core}} \tag{11}$$

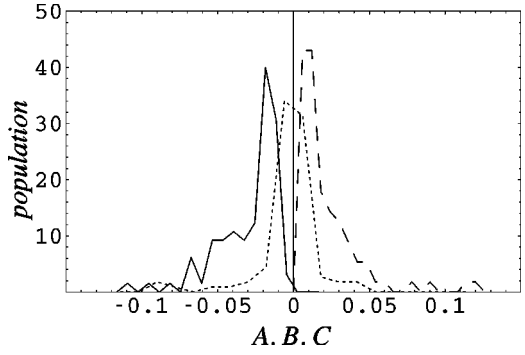

FIG. 2. Distribution of the parameters $A(\epsilon\sigma^{-2})$, solid line, $B(\epsilon\sigma^{-3})$, dotted line, $C(\epsilon\sigma^{-4})$, dashed line of the fitting potential $U^*(x)$ for the partial potential energy, $\langle U(x)\rangle_{\text{core}}$, for the 93 soft modes with participation ratio $p<0.25$.

(dotted line in Fig. 1).

We find for the soft modes that the double-well behavior is the rule for the potential energy of the core. This is clearly shown in the distribution of the soft potential parameters A,B,C, obtained for the 93 low-frequency modes with participation ratios $p<0.25$ found in our 55 glass configurations, see Fig. 2. Nearly the entire distribution of A values is on the negative side, which corresponds to double-well potentials. The rapid drop of the distribution of A for $|A|\rightarrow 0$ is in accord with the singularity $[p(A)\propto|A|]$ of the distribution of the harmonic force constants in the soft potentials. The corresponding distribution functions for the full potential energies of the modes has been given earlier.[8] Corresponding to the soft single wells found for the potential energy, summed over all atoms (Fig. 1), there the distribution with its singularity was observed on the side of positive A values. The partial potential energy, averaged over the 93 soft modes, is shown in Fig. 3. Note that the mean absolute value of the force constants A of the core potential is much larger than the force constant for the whole mode, which does not exceed, for the considered 93 modes, the value $A\simeq 0.0015\epsilon/\sigma^2$. This means that there is a very fine equilibration between the unstable core of a localized mode and the rest of the system. This equilibrium is very fragile, as can be seen from the close correlation between the eigenvectors of the soft modes and the direction of the relaxation ''jumps'' of atoms during annealing of the glass.[9,10]

As a next step we analyze the changes of the local structure produced by the collective displacements of the atoms.

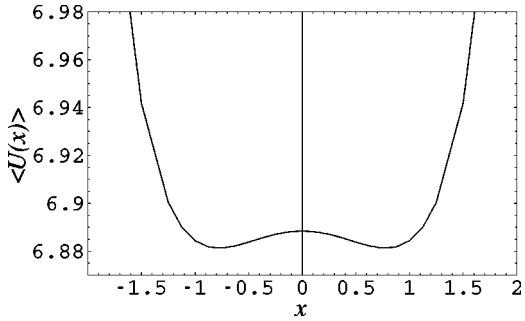

FIG. 3. Partial potential energy, $\langle U(x)\rangle_{\text{core}}$ averaged over the 93 soft modes. The curve is symmetrized because of the arbitrary sign of the normal coordinates.

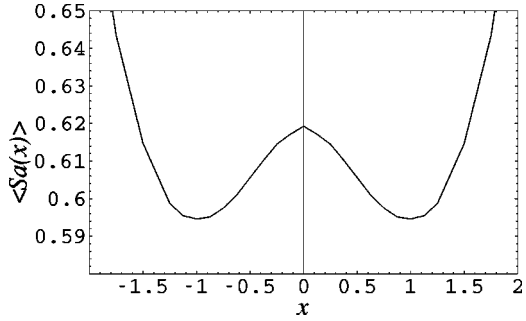

FIG. 4. Partial perfectness of atomic neighborhoods averaged over the 93 soft modes. The curve is symmetrized as in Fig. 3.

For each value of displacement x we repeat the tessellation of the atomic configuration into the Delaunay simplices and calculate the structure parameters defined in Sec. III. The most remarkable effect of the soft vibrations on the local structure is the marked and systematic increase of the number of perfect DS in the vicinity of the most active atoms for $x\approx\pm 1$. The new perfect simplices form those patterns of noncrystalline perfect structures, which are specific for the dense packings of spherical particles. In particular, we observe in the shifted configurations new five-fold rings of perfect tetrahedra. These rings are known to be the densest packings of seven equal spheres. This tendency is even more pronounced for the quart-octahedral DS, which form, in the shifted positions, new octahedra of almost perfect shape, which are connected to each other and to the tetrahedral DS so that new patterns of noncrystalline perfect structure appear. Those tetrahedra and quart-octahedra, which exist already at $x=0$, also increase their perfectness, i.e., their values T and O decrease as the configuration is shifted to the minima of the potential energy.

As done for the potential energy we calculate the average atomic perfectness $\langle S_{\text{atomic}}(x)\rangle_{\text{core}}$, Eq. (6), of the core, averaging over the same 93 soft modes. This average is shown in Fig. 4, that displays again a double-well form. Corresponding to Eq. (11) we do a least-square fit by a fourth-order polynomial,

$$\langle S^*_{\text{atomic}}(x)\rangle_{\text{core}}=A'x^2+B'x^3+C'x^4+\langle Sa(0)\rangle_{\text{core}}. \tag{12}$$

The distribution of the fitting coefficients A',B',C' is presented in Fig. 5. It is very similar to the distribution of the

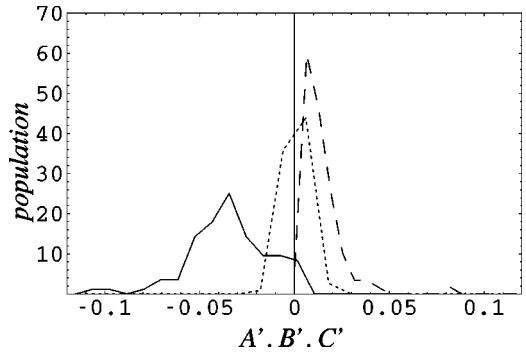

FIG. 5. Distribution of the parameters A'(solid line), B' (dotted line), C' (dashed line), for the fitting potential $S^*_{\text{atomic}}(x)$ of the partial perfectness of the atomic neighborhoods.

TABLE II. Average number of atoms in the core of the modes and average values of the parameters of the fitting potential $U^*(x)$ for the partial potential energy. The mean square deviations are given in parentheses.

	$\nu \leqslant 0.11$	$\nu \simeq 1.0$	$\nu \geqslant 1.85$
$\langle N_{\mathrm{core}} \rangle$	52	310	55
$A \quad (\epsilon\sigma^{-2})$	$-0.040(0.068)$	0.095(0.005)	1.62(0.53)
$\lvert B \rvert \quad (\epsilon\sigma^{-3})$	0.012(0.022)	0.0023(0.0021)	0.19(0.09)
$C \quad (\epsilon\sigma^{-4})$	0.030(0.056)	0.0015(0.0003)	0.54(0.40)

soft potential parameters for the partial potential energy (Fig. 2), and shows also a double-well behavior for the great majority of the fitting potentials.

Since the perfectness is given by a weighted sum of tetrahedricity, Eq. (2), and octahedricity, Eq. (3), it is interesting to repeat the above procedure for both components separately. Doing this one finds in the representation of Fig. 4 for the tetrahedricity a single well and for the octahedricity a more pronounced double-well behavior. The perfectness follows the potential energy more closely. We will meet this behavior again in the next section.

We can do the same representation for the atomic stresses.[48] We find for both the hydrostatic pressure p and the von Mises shear, τ, very flat wells with perhaps a hint of a double minimum. However, the absolute values of both these quantities for $x=0$ do not indicate so strongly the low-frequency quasilocalized modes. We get for these modes average frequency modes ($\nu \approx 1$) and high-frequency localized modes as average values $p=7.21$, 7.17, 7.44 and $\tau = 0.485$, 0.454, and 0.558, respectively. This shows that the high-frequency localized modes are clearly centered in high stress regions. For their low-frequency counterparts this is true to a much lesser extent.

We emphasize that the found double-well behavior, both for the core potential energy and the perfectness of the neighborhood of the active atoms, is specific to the quasilocalized low-frequency modes. For comparison, we have analyzed 70 modes in the middle-frequency and the high-frequency bands of the energy spectrum. The middle-frequency modes are delocalized: the average number of atoms that belong (for our definition) to the core of the mode is 310 (62% of all atoms). The high-frequency modes are again strongly localized, with the number of atoms in the core equal to 55. The average values of the fitting parameters for the partial potential energy and partial atomic perfectness are collected in Table II and Table III for the three types of modes (low-, middle-, and high-frequency modes). The small negative values of the coefficients C' for the partial perfectness of medium- and high-frequency modes are an artifact of the fitting procedure. Their smallness reflects the dominance of the harmonic term.

We propose the following interpretation of our results. In the glass of spherical soft particles, the landscape of the partial potential energy, calculated for the neighboring atoms, strongly correlates with such local structural parameter as the perfectness of the atomic packing. This gives a hint of the condition on the local structure where a soft vibration can arise. The core of the soft modes should consist of atoms that are in an intermediate position between two different realizations of local perfect packing. This is in agreement with calculations using random force constants in a coherent potential approximation where it was found that the boson peak appears as a precursor of instability.[49] But the perfectness of the atomic neighborhood is a purely geometrical characteristic. The statistics of the perfect and imperfect configurations, defined in terms of the tetrahedral and quart-octahedral Delaunay simplices, should be, in principle, universal for all close random packings of spherical particles, irrelevant to their physical nature. Thus we establish a connection between the universal geometrical properties of a system of spherical atoms and the peculiarities of its low-frequency dynamics. However, this conclusion is preliminary and has to be checked by further research.

V. CORRELATION BETWEEN STRUCTURE AND VIBRATION

We have seen that low-frequency quasilocalized vibrations have a specific impact on the structure surrounding the most active atoms of the vibration. We will now investigate how far a general relationship between structural measures and dynamics can be seen. We will concentrate here on tetrahedricity, Eq. (2). Qualitatively, we find the same trends also for perfectness, Eq. (5), and sphericity, Eq. (7).

As a first possible relation between structural measures and vibrations one can take the atomic tetrahedricity weighted by the amplitudes on the atoms. This would show whether e.g., atoms with low values of T_{atom} participate particularly strongly in vibrations in some frequency range. We define

TABLE III. Average number of atoms in the core of the modes and average values of the parameters of the fitting potential $Sa^*(x)$ for the partial perfectness of atomic neighborhood.

	$\nu \leqslant 0.11$	$\nu \simeq 1.0$	$\nu \geqslant 1.85$
A'	$-0.035(0.025)$	0.073(0.004)	0.39(0.14)
$\lvert B' \rvert$	0.003(0.003)	0.0010(0.0007)	0.052(0.038)
C'	0.013(0.011)	$-0.0005(0.0004)$	$-0.22(0.20)$

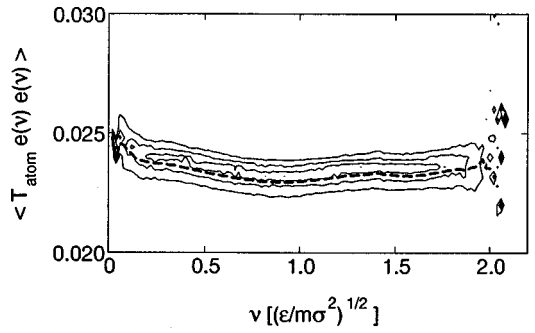

FIG. 6. Amplitude weighted atomic tetrahedricity as function of vibrational frequency mean value (dashed line) and equidistant contour lines.

$$T(\nu)=\left\langle \frac{1}{N}\sum_{n} T^{n}_{\text{atomic}}\mathbf{e}^{n}(\nu)\mathbf{e}^{n}(\nu)\right\rangle, \tag{13}$$

where $\mathbf{e}^n(\nu)$ stands for the three components, on atom n, of a vibrational eigenvector to frequency ν and $\langle\cdots\rangle$ denotes averaging over configurations and eigenvectors to similar frequencies. Taking the average value, the dashed line in Fig. 6, one observes only a slight variation with frequency. Only at the smallest frequencies is a small upturn found. The contour plot shows that the $T(\nu)$ values fall in general into a narrow band. This is different for the high-frequency localized modes $[\nu>2(\epsilon/m\sigma)^{1/2}]$. These modes have a large spread of $T(\nu)$ values without a clear preference for large or low atomic tetrahedricities. This large spread is a direct consequence of the strong localization, even to single atoms. The low-frequency modes always involve larger numbers of atoms, from 10 upwards, and, therefore, average over many different atomic tetrahedricities.

In the previous section we noted a connection between low-frequency vibrations and changes of structural elements. In order to quantify this notion we will now treat the average tetrahedricity, Eq. (8), as a structural potential and in analogy to the usual dynamic matrix define a *tetrahedricity matrix*

$$\mathcal{T}^{mn}_{\alpha\beta}=\frac{\partial^2\langle T\rangle}{\partial R^m_\alpha \partial R^n_\beta}. \tag{14}$$

Diagonalization of this matrix gives the eigenmodes of tetrahedricity change and the corresponding eigenvalues, which we will denote by $\mathbf{e}_\mathrm{T}$ and λ_T, respectively. To keep in line with the vibrations we use a tetrahedricity frequency $\nu_\mathrm{T}=\sqrt{\lambda_\mathrm{T}}/2\pi$.

In analogy to Eq. (13), where we defined an amplitude weighted tetrahedricity as function of frequency, we calculate the expectation value of the tetrahedricity matrix with respect to the vibrations, i.e., an amplitude weighted structural curvature,

$$\langle e(\nu)\mathcal{T}e(\nu)\rangle=\left\langle \sum_{\alpha\beta}^{mn} e^m_\alpha(\nu)\mathcal{T}^{mn}_{\alpha\beta}e^n_\beta(\nu)\right\rangle. \tag{15}$$

This expectation value shows several interesting features (Fig. 7). Most obviously there is a clear more or less linear increase with frequency. This linearity breaks down at the lowest frequencies $\nu<0.2(\epsilon/m\sigma)^{1/2}$, i.e., in the frequency range of the boson peak, where we find a distinct upturn.

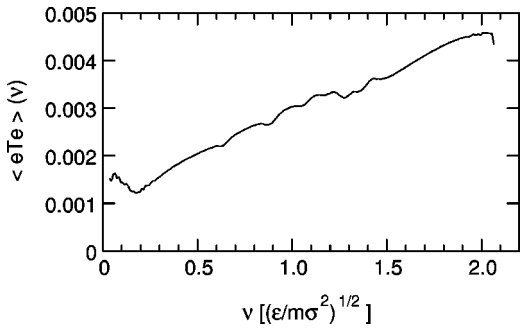

FIG. 7. Expectation value of tetrahedricity with respect to vibration modes versus frequency.

This upturn corresponds to the one in Fig. 6 but is much more pronounced. It clearly indicates a structural difference of the excess modes in the boson peak. It should be remembered that translational invariance requires $\langle e(\nu)\mathcal{T}e(\nu)\rangle \to 0$ for $\nu\to 0$. For a pure translation we get of course zero. Due to the limited system size, sound waves below $\nu<0.2(\epsilon/m\sigma)^{1/2}$ were eliminated and we do not see the increase towards this ''structural boson peak'' on the low-frequency side. The small dips of the curve for $\nu(\epsilon/m\sigma)^{-1/2}\approx 0.62, 0.88, \ldots$. coincide with the frequencies of the longitudinal sound waves in the SSG.

To get some deeper insight into the interplay of vibration and structure change we calculate the correlation matrix between the vibrational eigenmodes and their tetrahedricity counterparts

$$\langle e(\nu)e_\mathrm{T}(\nu_\mathrm{T})\rangle=\left\langle \sum_{n\alpha} (e^n_\alpha(\nu)e^n_{\mathrm{T}\alpha}(\nu_\mathrm{T}))^2\right\rangle. \tag{16}$$

The resulting correlation, Fig. 8, shows several interesting features. First there is a clear overall correlation as expected from Fig. 7. The correlation is highest for the highest-frequency modes. From the participation ratios[7] on can see that both vibrational and tetrahedricity modes are localized for the highest frequencies. For the great majority of modes two groups can be distinguished. The largest contribution

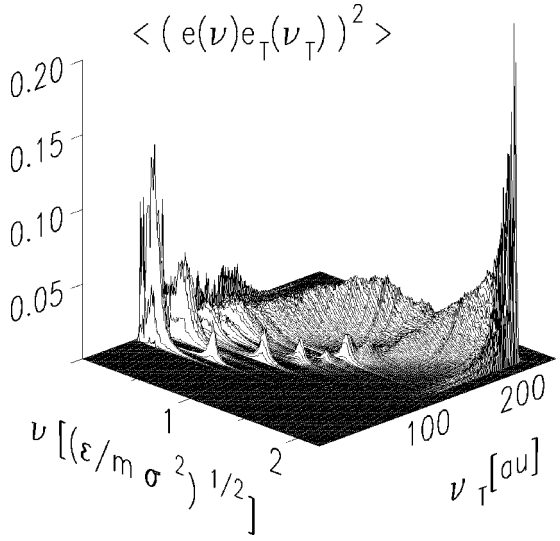

FIG. 8. Correlation of vibrational eigenvectors $\mathbf{e}$ and the eigenvectors $\mathbf{e}_\mathrm{T}$ of the tetrahedricity matrix as function of vibrational frequency ν and tetrahedricity frequency ν_T.

stems from a broad band stretching from the lowest ν values to the peak at the maximal ν values. In front of this band (higher ν values) there is a smaller one that can be identified as being due to longitudinal phonons that are well separated from the other vibrations in the SSG. A third group is seen as a narrow ridge at low ν covering a major part of the ν_T range. This last feature shows again the difference between the quasilocalized low-frequency modes and the rest of the spectrum. In a larger system interaction will of course mix these features. This does not, however, change the underlying nature of the ''naked'' modes.[8] Figure 8 does not only shows separate peaks for the longitudinal phonons permitted by the system size, but also in the ν_T direction separate ''phonons'' are seen, both transversal and longitudinal. Checking the participation ratios of e_T, one finds all modes with low ν_T extended and, therefore, no low-frequency localized modes are seen. The observed correlation is insufficient to predict localization at low frequencies. This is not too surprising as it has been observed earlier[7] that these modes are produced by a subtle interplay of local compression and in addition a resulting soft direction in configurational space involving several atoms. The tetrahedricity reproduces the first feature seen in the high-frequency modes, but not the second one.

We repeated the above calculation for the other measures introduced in Sec. III. The strong correlation between the vibrational and the ''structural'' eigenvectors proves to be stable against the choice of structural measure. The ''structural frequencies,'' on the other hand, vary quite strongly. In particular taking the ''perfectness'' defined by Eq. (5) some eigenvalues of the perfectness matrix, analogous to Eq. (14), become negative. One can tune the weights of tetrahedricity and octahedricity in Eq. (5) to move the smallest eigenvalues to positive values. This way one can produce also low-frequency localized structural modes that are correlated to their vibrational counterparts. Without an independent argument for such a weighting, this would, however, be a purely *ad hoc* definition.

VI. CONCLUSION

We have shown that the Voronoi-Delaunay geometrical approach gives an insight into the geometrical effects underlying the vibrations in the glass. For this purpose we introduced different measures to quantify the local environments: tetrahedricity, octahedricity, sphericity, and perfectness, derived from the first two. The idea of this perfectness is to fill space by distorted tetrahedra and octahedra. Perfectness is zero for the perfect shapes.

In real space the lowest-frequency quasilocalized vibrations can be envisaged as being caused by an instability of the local geometry that is stabilized by the embedding lattice. A group of atoms is trapped between two configurations that can be considered as more perfect using the above measure. Using the different measures one gets qualitatively the same picture. Instead of a double-well situation one frequently finds very flat single wells. For the higher-frequency modes we do not see such geometrically unstable cores. All our geometrical measures give single wells getting steeper with increasing frequency of the vibrations.

This picture of geometrical instabilities is related to the one of geometrical frustration.[34] Similar effects have recently been reported in a Lennard-Jones-type glass where it has been shown that there is a cancellation of positive and negative energy changes of the atoms along the mode.[50] This is in agreement with model calculations where the soft quasilocalized modes were seen as precursors of instability.[49] The atomic stresses[48] averaged over the core of the modes give very flat single-well potentials. The exact shape will, however, depend somewhat on the definition of the core of the vibration. For the higher-frequency modes no such unstable core was observed for our geometrical measures.

For the great majority of modes there is only a weak correlation between the amplitude they have on a single atom and the perfectness of this atom. This reflects the delocalization of the modes. The high-frequency localized modes that are concentrated on one or two atoms show a large scatter of their geometrical parameters, which indicates that they are caused by different local distortions. At the low-frequency side there is a small increase of tetrahedricity or perfectness that is, however, masked by the width of the distribution.

Clear correlations can be found between the curvatures in our structural landscapes and the vibrations. To show this we introduced structural dynamic matrices and calculated first the expectation values of these matrices with the vibrational eigenvectors. These values increase clearly with frequency and show some indication of a boson peak. In a second step we calculated the correlation between the structural and vibrational eigenvectors. These correlations divide the vibrations clearly into four different groups. First there are two bands of extended modes, longitudinal and transverse. The clear separation of these two bands is due to the large difference in longitudinal and transverse sound velocity for the considered soft-sphere glass. The high-frequencies localized vibrations are distinguished by the maximal correlation to the high-frequency structural modes. At the lowest frequencies, the region of the boson peak, the vibrations show again a distinctly different correlation behavior, indicating their structural origin. These modes are, for all geometrical measures we used, clearly separated from the bands of extended modes. This is a strong indication that they are to be considered as a separate species and not as some low-lying branch.

The qualitative picture is independent of the geometrical measure used (perfectness, tetrahedricity, or sphericity). Localization of low-frequency modes in structure space, however, is a much more subtle question. As in real space, localization of a resonant mode strongly depends on its frequency and so it does in our ''structural space.'' This frequency depends strongly on fine details as can be shown by changing the weights in the structural measure used. Using a suitable weighting of octahedricity and tetrahedricity one can define low-frequency structural modes that are correlated to the low-frequency quasilocalized (resonant) modes. This shows that these modes result from a very fine interplay of the structural entities involved in soft closed-packed random systems. A slight change can destabilize resonant modes or push them into the frequency band where they merge with the extended modes.

ACKNOWLEDGMENTS

One of the authors (V.A.L.) gratefully acknowledges the hospitality and financial support of the Forschungszentrum Jülich.

[1] *Amorphous Solids: Low Temperature Properties*, edited by W.A. Phillips (Springer-Verlag, Berlin, 1981).
[2] V.G. Karpov, M.I. Klinger, and F.N. Ignatiev, Zh. Éksp. Teor. Fiz **84**, 760 (1983) [Sov. Phys. JETP **57**, 439 (1983)].
[3] M.A. Il'in, V.G. Karpov, and D.A. Parshin, Zh. Eskp. Teor. Fiz **92**, 791 (1987) [Sov. Phys. JETP **65**, 165 (1987)].
[4] U. Buchenau, Y.M. Galperin, V.L. Gurevich, and H.R. Schober, Phys. Rev. B **43**, 5039 (1991).
[5] U. Buchenau, Yu. M. Galperin, V.L. Gurevich, D.A. Parshin, M.A. Ramos, and H.R. Schober, Phys. Rev. B **46**, 2798 (1992).
[6] V.L. Gurevich, D.A. Parshin, J. Pelous, and H.R. Schober, Phys. Rev. B **48**, 16 318 (1993).
[7] B.B. Laird and H.R. Schober, Phys. Rev. Lett. **66**, 636 (1991); H.R. Schober and B.B. Laird, Phys. Rev. B **44**, 6746 (1991).
[8] H.R. Schober and C. Oligschleger, Phys. Rev. B **53**, 11 469 (1996).
[9] H.R. Schober, C. Oligschleger, and B.B. Laird, J. Non-Cryst. Solids **156**, 965 (1993).
[10] C. Oligschleger and H.R. Schober, Phys. Rev. B **59**, 811 (1999).
[11] V.N. Novikov and N.V. Suretsov, Phys. Rev. B **59**, 38 (1999).
[12] J. Fabian and P.B. Allen, Phys. Rev. Lett. **79**, 1885 (1997).
[13] W. Jin, P. Vashishta, R.K. Kalia, and J.P. Rino, Phys. Rev. B **48**, 9359 (1993).
[14] C. Oligschleger and H.R. Schober, Physica A **201**, 391 (1993).
[15] J. Hafner and M. Krajci, J. Phys.: Condens. Matter **6**, 4631 (1994).
[16] P. Ballone and S. Rubini, Phys. Rev. B **51**, 14 962 (1995).
[17] L.D.V. Ee, B.J. Thijsse, and J. Sietsma, J. Non-Cryst. Solids **205-207**, 641 (1996).
[18] M. Cho, G.R. Fleming, S. Saito, I. Ohmine, and R.M. Stratt, J. Chem. Phys. **100**, 6672 (1994).
[19] J. Hafner and M. Krajci, J. Phys.: Condens. Matter **5**, 2489 (1993).
[20] S.N. Taraskin and S.R. Elliott, Phys. Rev. B **56**, 8605 (1997).
[21] C. Mascivecchio, V. Mazzacurati, G. Monaco, G. Ruocco, T. Scopigno, F. Sette, P. Benassi, A. Cunsolo, A. Fontana, M. Krisch, A. Mermet, M. Montagna, F. Rossi, M. Sampoli, G. Signorelli, and R. Verbeni, Philos. Mag. B **79**, 2013 (1999).
[22] A.P. Sokolov, R. Calemczuk, B. Salce, A. Kisliuk, D. Quitmann, and E. Duval, Phys. Rev. Lett. **78**, 2405 (1997).
[23] J. Fabian and P.B. Allen, Phys. Rev. Lett. **77**, 3839 (1996).
[24] M. Foret, E. Couretens, R. Vacher, and J.-B. Suck, Phys. Rev. Lett. **77**, 3831 (1996).
[25] P. Benassi, M. Krisch, C. Masciovecchio, G. Monaco, G. Ruocco, F. Sette, and R. Verbini, Phys. Rev. Lett. **77**, 3835 (1996).
[26] R. Dell'Anna, G. Ruocco, M. Sampoli, and G. Viliani, Phys. Rev. Lett. **80**, 1236 (1998).
[27] S.R. Elliott, Nature (London) **354**, 445 (1991).
[28] V.K. Malinovskii, V.N. Novikov, and A.P. Sokolov, Usp. Fiz. Nauk **163**, 119 (1993) [Phys. Usp. **163**, 440 (1993)].
[29] S.-P. Chen, T. Egami, and V. Vitek, Phys. Rev. B **37**, 2440 (1988).
[30] T. Egami, J. Mater. Sci. **13**, 2587 (1978).
[31] T. Kustanovich and Z. Olami, Phys. Rev. B **61**, 4813 (2000).
[32] R. Jullien, P. Jund, D. Caprion, and J.-F. Sadoc, in *Physics of Glasses*, edited by P. Jund and R. Jullien, AIP Conf. Proc. No. 489 (AIP, Melville, NY, 1999), p. 129.
[33] J.-F. Sadoc and R. Mosseri, *Geometrical Frustration* (Cambridge University Press, Cambridge, 1999).
[34] T. Egami, Mater. Sci. Eng., A **226**, 261 (1997).
[35] J.M. Ziman, *Models of Disorder: The Theoretical Physics of Homogeneously Disordered Systems* (Cambridge University Press, Cambridge, 1979), Chap. 11.
[36] P.H. Dederichs and R. Zeller, *Point Defects in Metals II*, Springer Tracts in Modern Physics Vol. 87 (Springer-Verlag, Berlin, 1980).
[37] P. Ehrhart, K.H. Robrock, and H.R. Schober, in *Physics of Radiation Defects in Crystals*, edited by R.A. Johnson and A.N. Orlov (North-Holland, Amsterdam, 1986), p. 3.
[38] N.N. Medvedev, Y.I. Naberukhin, and V.A. Luchnikov, J. Struct. Chem. **35**, 47 (1994).
[39] V.A. Luchnikov, N.N. Medvedev, Y.I. Naberukhin, and V. Novikov, Phys. Rev. B **51**, 15 569 (1995).
[40] P. Jund, D. Caprion, and R. Jullien, Phys. Rev. Lett. **79**, 91 (1997).
[41] W.G. Hoover, S.G. Gray, and K.W. Johnson, J. Chem. Phys. **55**, 1129 (1971).
[42] D. Caprion, P. Jund, and R. Jullien, Phys. Rev. Lett. **77**, 675 (1996).
[43] P. Jund, D. Caprion, and R. Jullien, Europhys. Lett. **37**, 547 (1997).
[44] N.N. Medvedev and Y.I. Naberukhin, J. Comput. Phys. **67**, 223 (1986).
[45] N.N. Medvedev, J. Phys.: Condens. Matter **2**, 9145 (1990).
[46] V.P. Voloshin, N.N. Medvedev, and Y.I. Naberukhin, Mol. Simul. **4**, 209 (1989).
[47] N.N. Medvedev and Y.I. Naberukhin, J. Non-Cryst. Solids **94**, 402 (1987).
[48] T. Egami and S. Aur, J. Non-Cryst. Solids **89**, 60 (1987).
[49] G.D.W. Schirmacher and C. Ganter, Phys. Rev. Lett. **81**, 136 (1998).
[50] L. Angelani, M. Montagna, G. Ruocco, and G. Viliani, Phys. Rev. Lett. **84**, 4874 (2000).